NASF SURFACE TECHNOLOGY WHITE PAPERS
80 (3), 13-28 (December 2015)

The Behavior of Intermetallic Compounds in Aluminum during Sulfuric Acid Anodizing
Part 2: Al-Cu, Al-Mg, Al-Si, Al-Ti, Al-Fe-Si, Al-Zn-Mg Alloys

by
J. Cote,[1] E.E. Howlett[1] and H.J. Lamb[2]
[1]Alcan Research and Development, Ltd., Kingston, Ontario, Canada
[2]Alcan Research and Development, Ltd., Banbury, England, U.K.

Editor's Note: This paper was originally published as J. Cote, *et al*., *Plating*, 57 (5), 484-496 (1970).

ABSTRACT

The behavior of coarse particles of five intermetallic compounds, $CuAl_2$, beta AlMg, Si, $TiAl_3$, beta AlFeSi and the T (AlZnMg) phase** in high purity based aluminum alloys, during sulfuric acid anodizing under constant d-c potential, has been examined using optical microscopy and electron probe microanalysis. Point analysis was used to identify the constituents and to measure compositions within the matrices and the anodic films while the ultra-slow scan technique was used to determine concentration profiles through the anodic films. Results are compared with those of other workers in this field. As expected, Si was inert as were $TiAl_3$ and beta AlFeSi while $CuAl_2$, beta AlMg, and the T (AlZnMg) phase were anodized faster than the matrix and readily dissolved in the electrolyte. Of the elements in solid solution, silicon was retained in the anodic film, zinc was partly soluble, while copper, iron, and magnesium dissolved in the electrolyte.*

Introduction

In an earlier paper,[1] we described the anodic behavior in sulfuric acid, under constant d-c potential, of a few large intermetallic compounds ($MnAl_6$, $FeAl_3$, Mg_2Si and $CrAl_7$) in high purity base aluminum alloys. These intermetallic compounds were respectively inert, anodized at the same rate, anodized faster, and readily dissolved in the electrolyte with respect to the matrix during the anodizing process. The anodic behavior of the intermetallic compounds was studied by making extensive use of an electron probe microanalyzer and its scanning backscatter electron and x-ray imaging systems. This tool proved very useful for the identification of intermetallic compounds (confirmed by x-ray diffraction technique) and for the quantitative analysis of intermetallic compounds, matrices and anodic films formed above them. Thus the concentration of the major alloying elements could be determined and, even with an accuracy of ± 5%, it was possible to establish whether or not the elements were retained in the anodic films.

The object of the present work is to describe the anodic behavior of another group of intermetallic compounds. The constituents were selected because of their common occurrence in various commercial aluminum alloys and because these constituents, through their anodizing characteristics, can influence the appearance and corrosion resistance of anodized products. The intermetallic compounds examined were $CuAl_2$, beta AlMg, Si, $TiAl_3$, beta AlFeSi and the T (AlZnMg) phase. Although the anodic behavior of these intermetallic compounds in either sulfuric acid or oxalic acid electrolytes has been reported by various workers,[2-8] further evidence was obtained which confirms or questions what has been previously found.

The behavior of alloying elements in solid solution in the aluminum matrix is of importance since this may affect, to some degree, the properties of anodic films. In some instances, a different anodizing response was observed depending upon whether the elements were in solid solution or formed intermetallic compounds.[1] Using a technique similar to that of Wood and Brock,[8] the distribution of alloying elements across matrix-anodic film was measured by the slow-scan of an electron probe microanalyzer. The behavior of elements in solid solution was then compared with other work where such behavior was determined by the x-ray fluorescence method.[9,10]

---

*Silicon particles are second phase constituents rather than intermetallic compounds, but for simplicity throughout the study, the latter term has been used.
**T (AlZnMg) phase, or more simply, and hereafter, T phase.

Experimental

The eight alloys investigated (Table 1) were prepared, as in our earlier work,[1] by melting super-purity aluminum (Alcan 99.99%) with the appropriate addition of commercially high purity elements: Cu (99.96%), Si (99.8%), Ti (99.99%), Mg (99.98%), Fe (99.92%), Zn (99.99%). Some of the alloys were cast (Table 1) in a preheated marinite mold, as used previously, so providing a slow cooling rate (1.5 to 4°C/min). However, in other cases, a medium cooling rate (20 to 30°C/min) was necessary because of (1) the too great solubility of alloying element in the matrix which prevented the formation of sufficiently large intermetallic compounds under slow cooling conditions or (2) to minimize peritectic reaction around intermetallic compounds. This was accomplished by using a preheated (400°C) steel mold designed to produce tapered round bar of 2.5 to 3.8 cm by 17.8 cm long (1 to 1.5 in. by 7 in.). The mold was coated with Mica Wash*** to give more uniform cooling conditions.

Table 1 - Casting conditions and spectrographic analyses of super-purity aluminum base alloys.

Alloy	Casting Temp. (C)	Cooling Condition	Per Cent Element by Weight							
			Cu	Fe	Mg	Mn	Si	Ti	Zn	Cr
Al-10Cu	734	Slow*	10.31	<0.01	<0.001	<0.001	<0.001	0.002	<0.01	0.002
Al-10Mg	830	Slow and Medium**	0.002	0.001	9.4	<0.001	0.002	<0.001	<0.001	<0.001
Al-13Si	760	Slow	0.001	0.05	<0.001	<0.001	12.21	<0.001	<0.001	<0.001
Al-1Ti	890	Medium	0.002	0.001	0.005	<0.001	0.01	0.82	0.008	<0.001
Al-4Fe-8Si	760	Slow	0.005	3.96	0.004	<0.001	8.87	<0.001	<0.001	<0.001
Al-9Mg-3Zn	856	Slow	<0.01	<0.01	8.76	<0.01	<0.01	<0.01	3.11	<0.01
Al-9Zn-3Mg	808	Slow	<0.01	<0.01	2.99	<0.01	<0.01	<0.01	9.23	<0.01

*1.5 to 4° C/min
**20 to 30° C/min

The Al-13Si alloy was investigated in both the as-cast and homogenized (16 hr at 555°C) conditions.

The specimen preparation, anodizing conditions in sulfuric acid electrolyte (15 wt%, 21°C) under constant d-c potential (16V), and procedures for metallographic and electron probe microanalysis examination were similar to those outlined previously.[1] In addition, in a few cases, the profile distribution of aluminum and the alloying elements through the anodic films formed above the matrix was carried out by using the ultra-slow scanning device of the electron probe microanalyzer.[8] All measurements were made at 20 KV.

Experimental results

A. Anodic behavior of intermetallic compounds

1. General

During the 30 min period of anodizing under constant potential, current flow for the individual specimen was recorded. The current varied from sample to sample but, as expected[11,12] was higher with aluminum-magnesium and aluminum-zinc-magnesium alloys with an apparent current density of about 3.2 A/dm^2 (30 A/ft^2) resulting in an anodic film 100 to 125 microns thick. The current flow on the other alloys was lower, being about 1.1 to 1.6 A/dm^2 (10-15 A/ft^2), which produces anodic film thicknesses of 6 to 25 microns depending on the alloy. With the Al-10% Cu alloy, a very thin film was formed owing probably to a lower current density[6] attributed, among other things, to increased ohmic resistance of the anodic film due to the presence of copper[11] (or copper oxides) and the lower anode current efficiency.[12] The analytical data obtained by electron probe microanalysis are summarized in Table 2. Wherever possible, the observed values have been corrected for x-ray absorption. For reasons explained elsewhere,[1] the corrected values did not add up to 100%. The elemental compositions of the anodic films of those particles which oxidized, and of the various aluminum matrices are also included in Table 2. In this case, no attempt to correct the composition in the anodic film for absorption effect was made because of inherent difficulties in measuring the oxygen content in the anodic films. However, the observed aluminum content of anodic films was within the range obtained by Wood, *et al.*[13] who used similar techniques.

*** Mica Wash No. 15, Springfield Facing Co., Springfield, Mass.

Table 2 - Electron probe microanalyses (20 kV) of the major alloying elements in the matrix, the intermetallic compounds and the anodic film above each.

			Element in Matrix or Intermetallic Compound (per cent by wt)			Element in Anodic Film (per cent by wt)
Alloy	Phase	Element	Observed	Corrected for Absorption	Stoichiometric*	Observed
Al-10Cu	Matrix	Cu	3.0	3.0		0.2
		Al		97.0 (diff.)		32.0†
	$CuAl_2$	Cu	48.5	50.0	54	NA**
	(dissolved)	Al	17.5	49.3	46	NA
Al-10Mg	Matrix	Mg	7.5	7.9		0.5
		Al		92.1 (diff.)		27
	Beta AlMg	Mg	29.5	30.5	36.1	NA
	(dissolved)	Al	28.6	73.4	63.9	NA
Al-13Si	Matrix	Si	0.6	~1.5		0.6
		Al		98.5 (diff.)		31
	Si	Si	~100	~100	100	NA
Al-1Ti	Matrix	Ti	trace			trace
		Al		~100		?
	$TiAl_3$	Ti	33	36.5	37.2	NA
	(inert)	Al	35	58.6	62.8	NA
Al-4Fe-8Si	Matrix	Fe	0.1	0.1		trace
		Si	0.5	1.5		0.5
		Al		98.4 (diff.)		31
	Beta AlFeSi	Fe	25.5	26.6	26–27	NA
	(inert)	Si	4.2	13.8	13–14	NA
		Al	30.3	53.6	59–61	NA
Al-9Mg-3Zn	Matrix	Mg	6.3	7.3		0.6
		Zn	2.1	2.1		0.5
		Al		90.6 (diff.)		28
	T (AlZnMg)	Mg	11.3	32.0		NA
	phase	Zn	20.0	23.0		NA
	(dissolved)	Al	12.7	45.0		NA
Al-9Zn-3Mg	Matrix	Zn	7.5	7.5		1.1
		Mg	1.3	1.9		trace
		Al		90.6 (diff.)		30
	T (AlZnMg)	Zn	42.5	42.0		NA
	phase	Mg	2.5	23.0		NA
	(dissolved)	Al	9.0	35.0		NA

*Values calculated on the proportional weight based on the stoichiometric ratio of the intermetallic compound.
†Variable concentration across anodic film.
**NA means not applicable.

The anodic behavior of each intermetallic compound is as described below.

2. $CuAl_2$

The slow cooled Al-10Cu alloy contained a mixture of primary crystals identified as $CuAl_2$ in addition to eutectic regions of $CuAl_2$-aluminum. Point analysis of $CuAl_2$, both as primary and eutectic particles contained, after correction, 50 wt% Cu (Table 2).

The anodic behavior of both primary and eutectic $CuAl_2$ is well illustrated in Fig. 1. The formation of a thin anodic film with this alloy can also be noted. Primary crystals of $CuAl_2$ (Fig. Ia) were rapidly oxidized and readily dissolved in the electrolyte and the cavity walls of the gradually dissolving particles were progressively oxidized. Anodizing of the $CuAl_2$-aluminum eutectic (Fig. Ib) also resulted in the rapid oxidation-dissolution of the $CuAl_2$ component although the aluminum component was also oxidized, but some segments of aluminum were electrically cut off from the eutectic network before they had been completely oxidized. In this manner, aluminum particles were retained in the oxide coating as are inert particles. The dissolution of the oxidized $CuAl_2$ particles resulted in production of small fresh areas which in turn are anodized and through which most of the current will flow. In all likelihood, the current density over the oxidized surface is therefore reduced. This effect might also have contributed in the formation of a thin anodic film with this alloy composition.

The optical micrograph, the corresponding electron scanning image, and the aluminum and copper Kα radiation x-ray scanning images for another particle of primary $CuAl_2$ are shown in Fig. 2. The oxidation of the cavity walls can be clearly noted in the

aluminum Kα radiation image (Fig. 2c). The oxidation of the intermetallic particles can be noted in Fig. 2d; this shows the copper concentration at the tip of the dissolving branches to be less than that in the bulk of the particle.

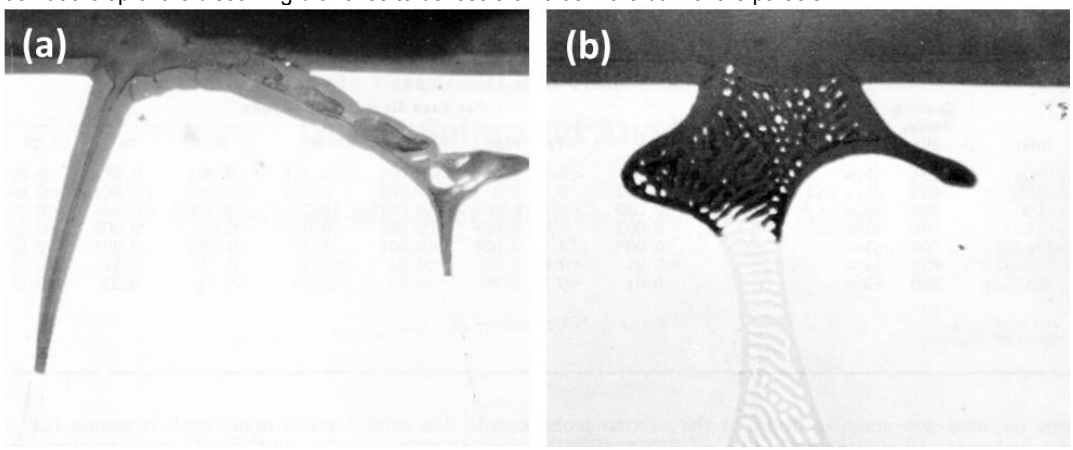

Figure 1 - Cross-section through anodized Al-10Cu alloy: (a) primary crystal of $CuAl_2$ (400×) and (b) eutectic $CuAl_2$-aluminum (500×).

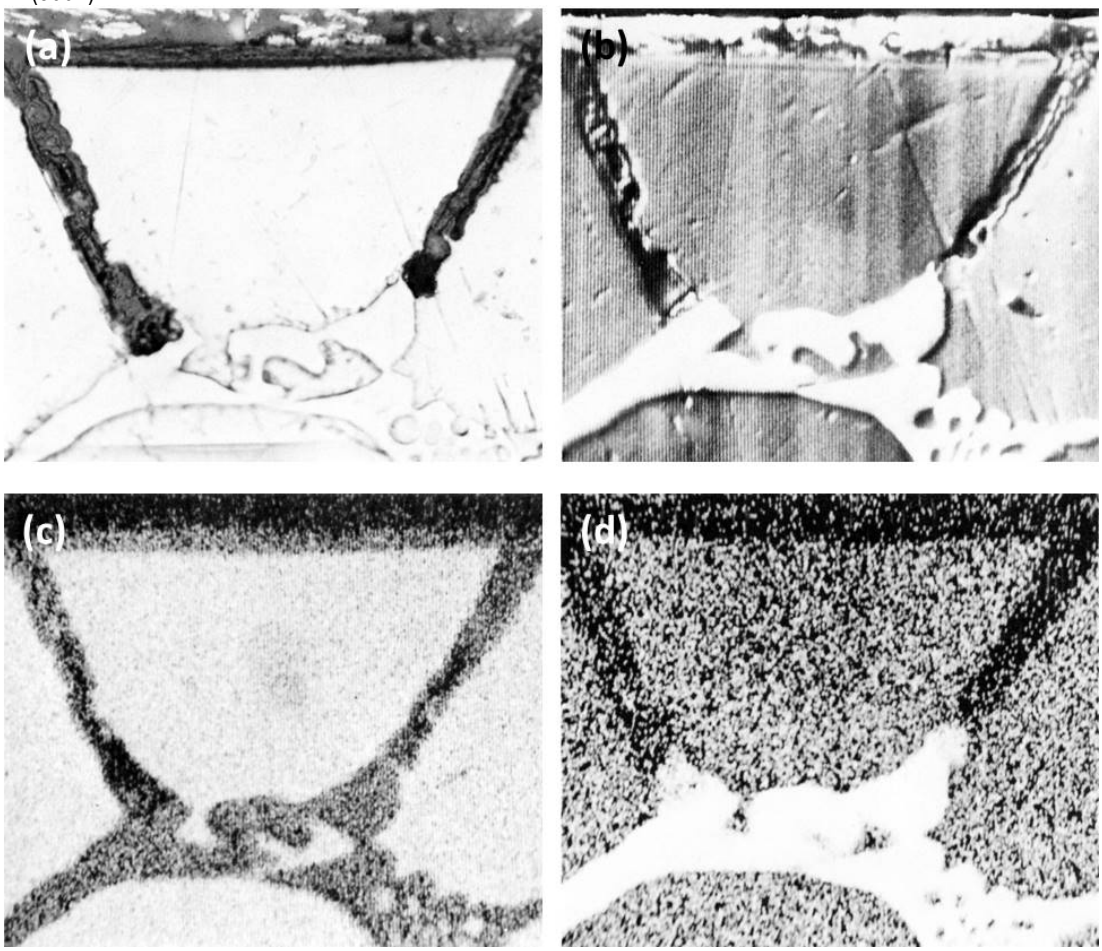

Figure 2 - Cross-section of anodized Al-10Cu alloy showing the behavior of primary $CuAl_2$ (Original magnification 500×): (a) optical micrograph, (b) electron scanning image, (c) Al Kα radiation x-ray scanning image and (d) Cu Kα radiation x-ray scanning image.

3. Beta AlMg

The slow cooled Al-10Mg alloy contained large irregularly shaped intermetallic particles identified as beta AlMg which is sometimes referred to as Mg_5Al_8 or Mg_2Al_3. Point analysis revealed that beta AlMg had a corrected value of 30.5 wt% magnesium while the matrix contained 7.9% magnesium (Table 2). As expected, in the metallographically as-polished condition, beta AlMg was hardly distinguishable[14] from the aluminum matrix (Fig. 3).

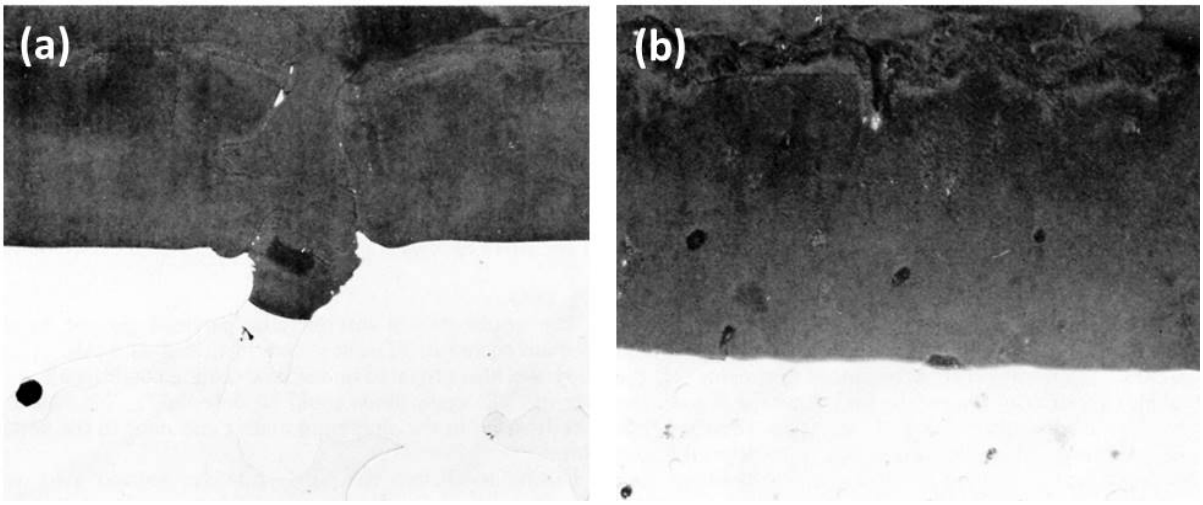

Figure 3 - Cross-section through anodized Al-10Mg alloy: (a) large beta AlMg crystals, slow-cooled (Original magnification 300×) and (b) small beta AlMg particles, medium-cooled (Original magnification 500×).

The beta AlMg constituents anodized at a slightly faster rate than the aluminum matrix and dissolved in the electrolyte, producing large discontinuities or voids in the anodic coating (Fig. 3a)(In these cases, the voids became filled with "Bostik" mounting lacquer.). Some scalloping of the metal/oxide interface near the crystal of beta AlMg has occurred and this is attributed to the current thieving.[15]

A similar alloy, cast under medium-cooling conditions, resulted in the formation of small spheroidal constituents also identified as beta AlMg. These were also anodized and dissolved during anodizing leaving holes in the anodic coating (Fig. 3b).

With both samples pronounced roughness resulted at the electrolyte/oxide interface as compared to a relatively smooth oxide/metal interface especially noticeable in Fig. 3b. The dissolution of the oxidized constituents appeared to be partly responsible for the formation of the irregular oxide/electrolyte interface.

The dissolution of beta AlMg compounds is confirmed by the Kα radiation x-ray scanning images (Fig. 4) of a beta AlMg particle. Here, the intermetallic particle is of similar mean atomic number to that of the matrix and hence is faintly visible on the electron image (Fig. 4b). Figures 4c and 4d show more clearly that the discontinuity in the anodic film is, in fact, a hole and that it appears that the beta AlMg compounds dissolved as fast as they were anodically oxidized.

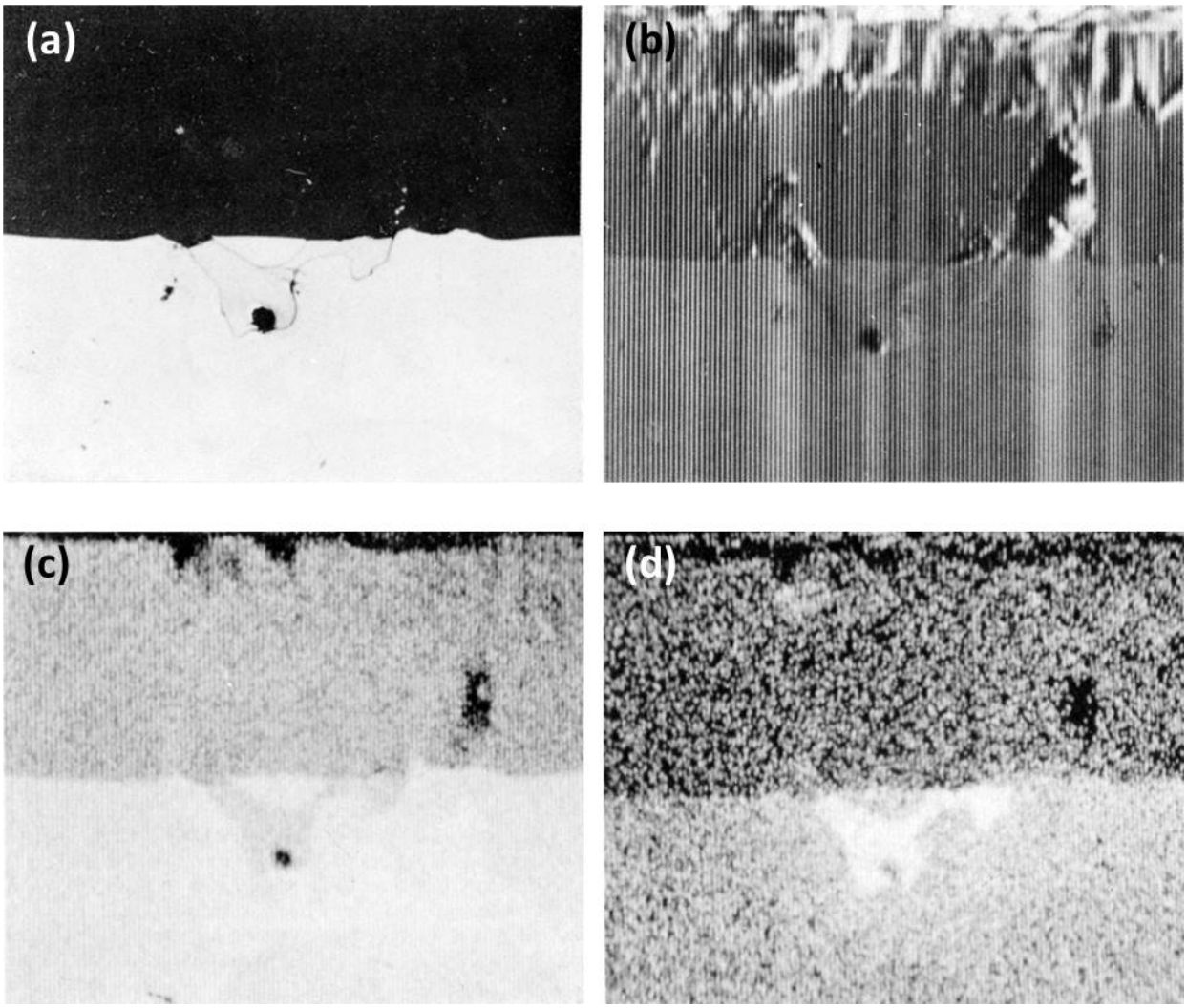

Figure 4 - Cross-section of anodized Al-10Mg alloy showing the behavior of beta AlMg (300×): (a) optical micrograph, (b) electron scanning image, (c) Al Kα radiation x-ray scanning image and (d) Mg Kα radiation x-ray scanning image.

The pronounced scalloping of the anodic film around the silicon particles occurred in both the as-cast and homogenized samples and was therefore not caused by coring. However, this effect, as mentioned in our earlier paper,[1] can be caused either by current thieving from the intermetallic compounds[15] or possibly, because of their apparent high electrical resistance, by the intermetallic particles acting as shields to the current flow. Figures 5a and 5b show a strong dependence of the scalloping of the anodic film with orientation of the silicon particles suggesting that current shielding rather than current thieving had taken place. Break-up of the silicon particles is also apparent, and this is almost certainly due to the silicon particles fracturing under the stresses developed by the expansion of the oxide film relative to the metal from which it has formed. It is possible, but considered very unlikely, that the break-up occurred during metallographic preparation.

The inertness of the Si constituents is quite evident from the series of the electron and aluminum and silicon Kα radiation x-ray scanning images, (Fig. 6), on another area of the Al-13Si alloy.

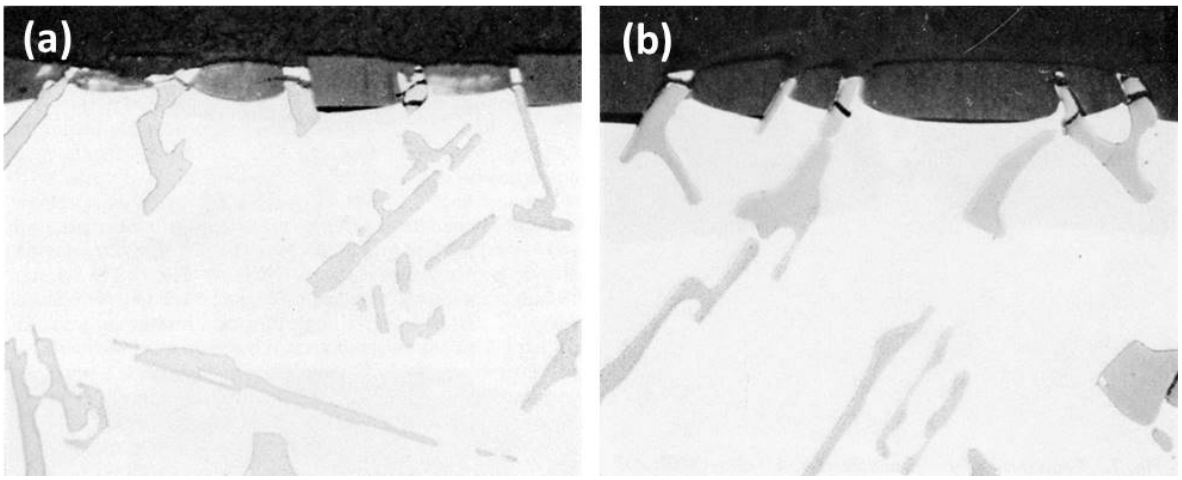

Figure 5 - Cross-section of anodized Al-13Si (500×): (a) as cast and (b) homogenized (16 hr at 555°C).

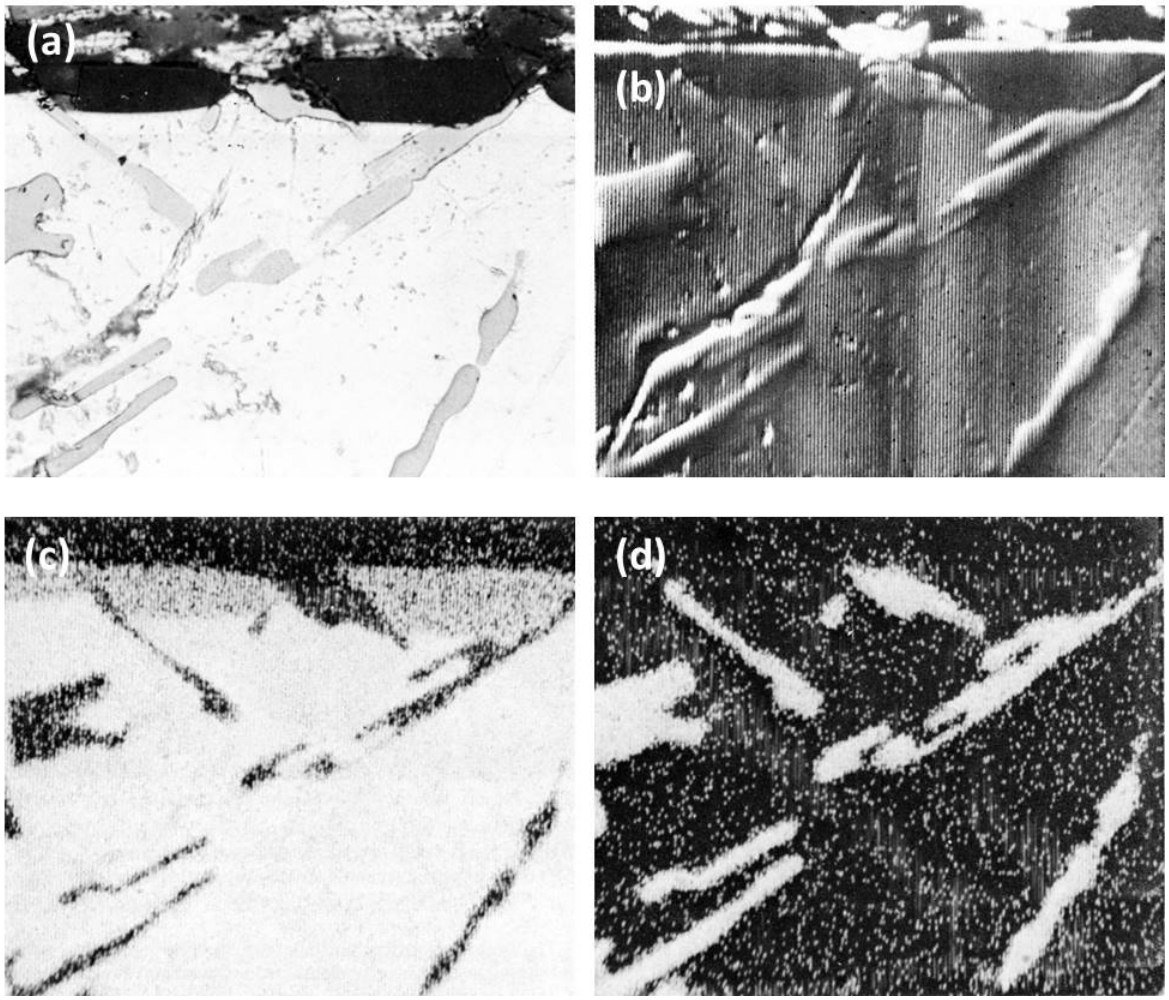

Figure 6 - Cross-section of anodized Al-13Si alloy illustrating the behavior of eutectic silicon (Original magnification 500×): (a) optical micrograph, (b) electron scanning image, (c) Al Kα radiation x-ray scanning image and (d) Si Kα radiation x-ray scanning image.

5. $TiAl_3$

The needle-shaped intermetallic particles present in the medium cooled Al-1 Ti alloy were identified as $TiAl_3$. (This alloy was also prepared under slow cooling conditions but no intermetallic compounds could be detected.†) No titanium was detected in the aluminum matrix and none in the anodic film.

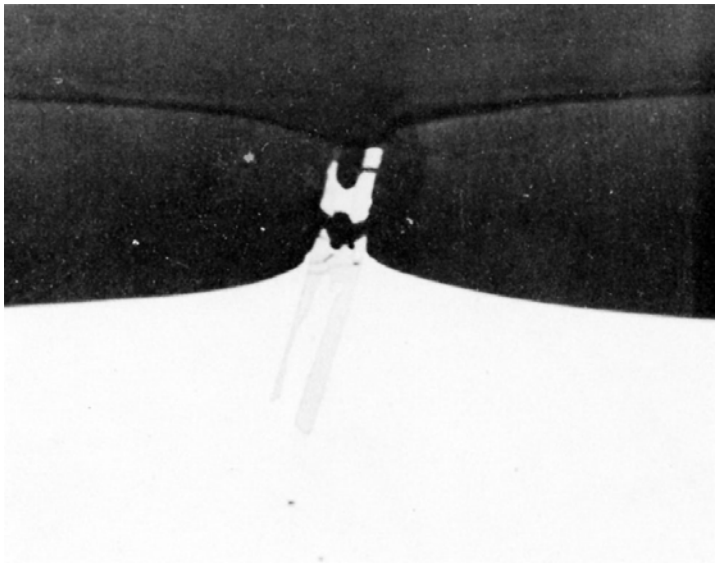

Figure 7 - Cross-section through anodized Al-1 Ti alloy (1000×).

During anodizing, the $TiAl_3$ particles seemed inert and were projected into the anodic film (Fig. 7) with "scalloping" of the anodic film taking place, around the particle, at the oxide/metal interface. Fracture of the needle-shaped $TiAl_3$ particle occurred in the anodic film, in the same manner as with silicon particles and presumably for the same reason. In Fig. 7, aluminum trapped between pieces of $TiAl_3$ remained unoxidized owing to electrical cut-off. This strongly suggests that fracture of the inert intermetallic compounds occurred during anodizing rather than during metallographic polishing. Further evidence of the inert behavior of the $TiAl_3$ particles is illustrated in the series of electron probe x-ray images (Fig. 8). Here it appeared that some thinning of the $TiAl_3$ needles could have taken place. This apparent thinning can be noted particularly on the left hand particle of $TiAl_3$ (Fig. 8d) but two slow scans across this particle, first where it projects into the film, and second where it is still embedded in the matrix, failed to reveal any titanium in the anodic film adjacent to the needle. This seems to indicate that if some slight dissolution of the $TiAl_3$ particles has occurred, the titanium was not retained in the film.

6. Beta AlFeSi

The Al-4Fe-8Si alloy was examined in both slow and medium cooled conditions. In the slowly solidified sample, large plates and small needles of beta AlFeSi were identified along with angular particles of eutectic silicon (Fig. 9a). In the medium cooled sample, small needle-shaped beta AlFeSi particles were present but there was little evidence of eutectic silicon (Fig. 9b). The observed point analysis of the beta AlFeSi compound gave the result (Table 2) of 25.5 wt% iron, 4.2 wt% silicon and 30.3 wt% aluminum. Correcting these figures according to Birks[16] gives 26.6 wt% iron, 13.8 wt% silicon and 53.6 wt% aluminum. However, experience with microanalysis of iron-aluminum intermetallic compound in this composition range indicates that the corrected iron figures are usually about 1 wt% low compared with the figures given by chemical analysis of the extracted crystals. Therefore, the exact iron content should be in the vicinity of 27.6 wt% iron. Based on the aluminum content, the Fe:Al ratio is roughly 1:2 and Si:Al is 1:4. In both samples, the corrected analysis matrix showed 0.1 wt% iron and 1.5 wt% silicon.

†Slow solidification approaching equilibrium conditions of a 1 wt% Ti alloy will produce an aluminum-rich solid solution at 665°C; on further cooling the $TiAl_3$ will precipitate. In our slow cooled alloy, no intermetallic particles could be detected and the $TiAl_3$ particles, if any, were too small to be noted.

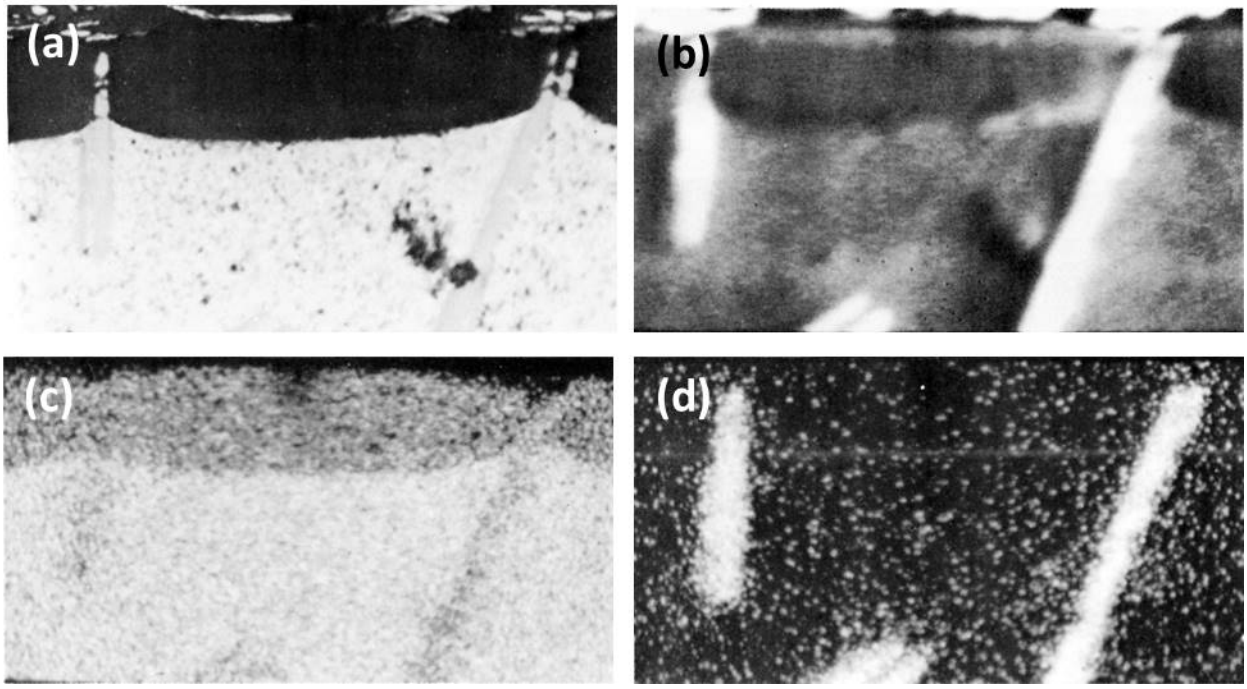

Figure 8 - Cross-section of anodized Al-1 Ti alloy illustrating the behavior of $TiAl_3$ (750×): (a) optical micrograph, (b) electron scanning image, (c) Al Kα radiation x-ray scanning image and (d) Ti Kα radiation x-ray scanning image.

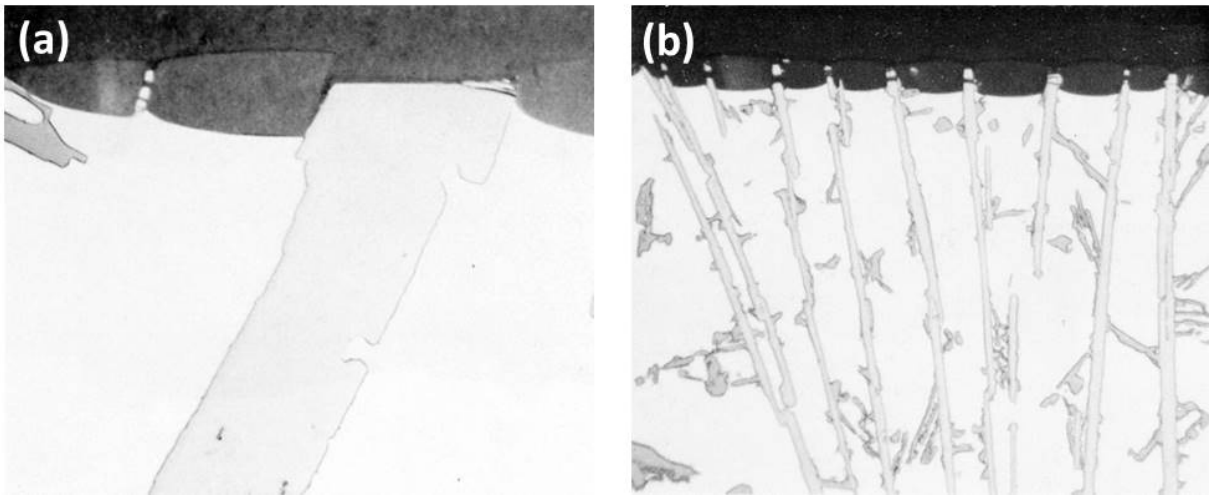

Figure 9 - Cross-section of anodized Al-4Fe-8Si alloy (500×): (a) large beta AlFeSi and eutectic silicon (upper left), (b) needles of beta AlFeSi, medium-cooled.

The beta AlFeSi particles were inert to anodic oxidation under the anodizing conditions used (Fig. 9). With the small needle-shaped particles (Fig. 9b), the portion protruding in the anodic film was broken-up. The "scalloping" of the anodic film around the inert particles occurred as with the other above inert intermetallic compounds. In Fig. 9a, a small particle of eutectic silicon was present (upper left) and as expected this was inert.

The series of optical and the corresponding electron scanning images and the aluminum, iron and silicon Kα radiation x-ray scanning images of another particle of beta AlFeSi are illustrated in Fig. 10. There was no indication that any kind of attack took place. The beta AlFeSi particle was totally inert.

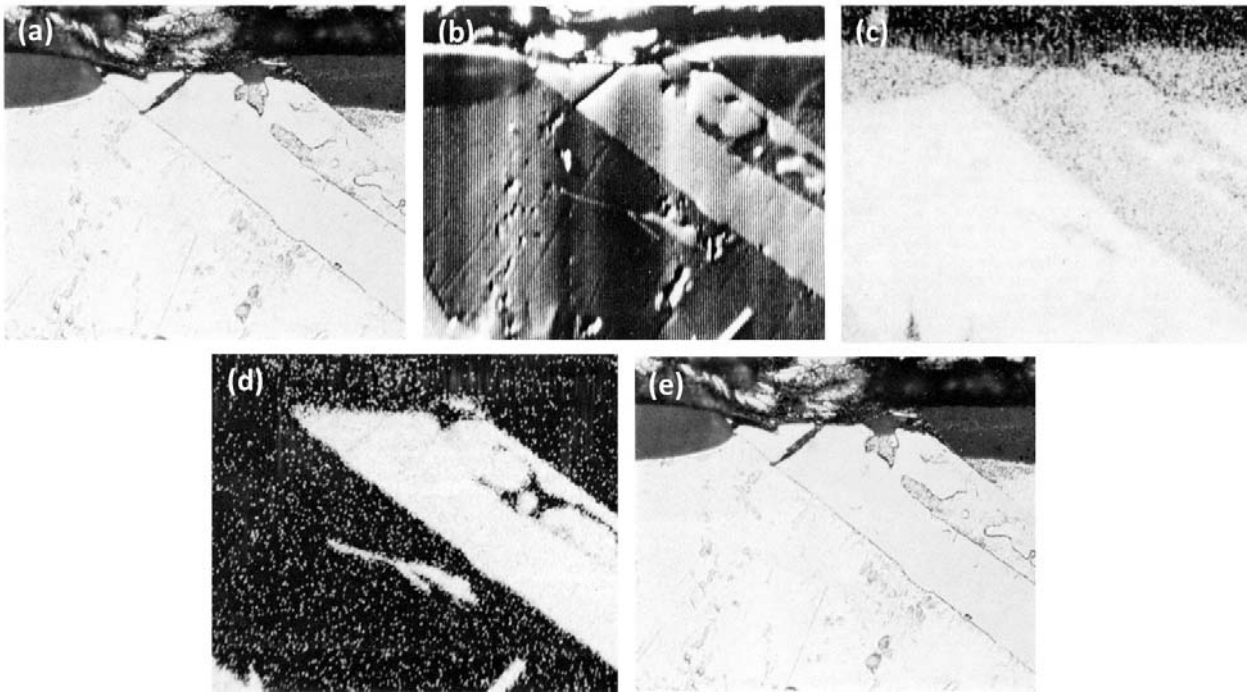

Figure 10 - Cross-section of anodized Al-4Fe-8Si alloy illustrating the behavior of AlFeSi (500×): (a) optical micrograph, (b) electron scanning image, (c) Al Kα radiation x-ray scanning image, (d) Fe Kα radiation x-ray scanning image and (e) Si Kα radiation x-ray scanning image.

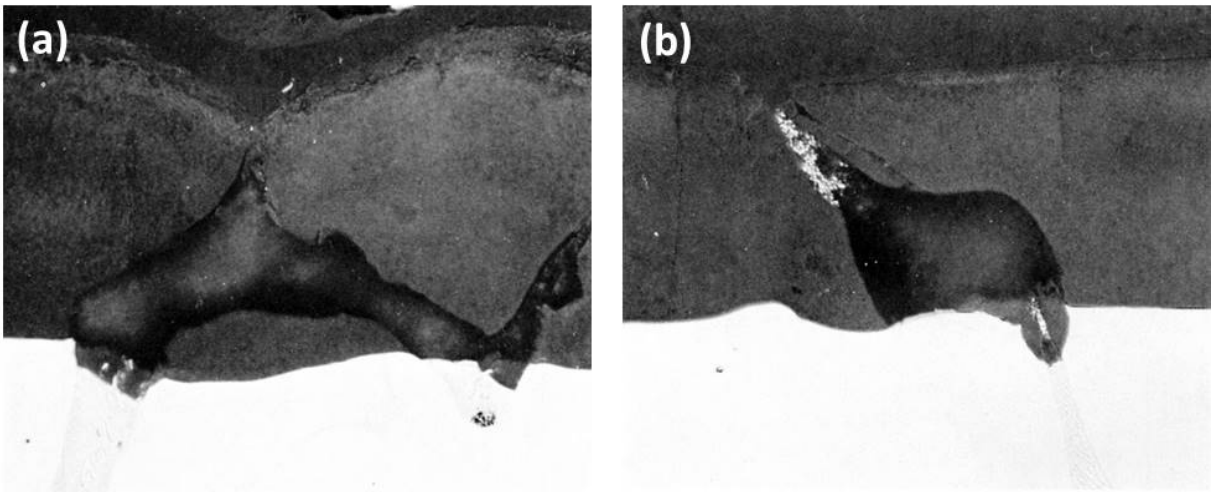

Figure 11 - Cross-section of anodized Al-Mg-Zn alloys (Original magnification 400×): (a) Al-9Mg-3Zn showing large particle of T phase and (b) Al-9Zn-3Mg showing eutectic of Al-T phase.

7. T (AlZnMg) phase

The only intermetallic compounds found in either of the slow-cooled Al-Zn-Mg alloys were identified as the T phase. In the Al-9Mg-3Zn alloy, irregularly-shaped crystals of the T phase were present (Fig. 11a), containing, after corrected electron probe microanalysis (Table 2), 32 wt% magnesium, 23 wt% zinc and 45 wt% aluminum. The corrected matrix analysis revealed 7.3 wt% magnesium and 2.1 wt% zinc. In the Al-9Zn-3Mg alloy, the only intermetallic compounds observed occurred in regions of eutectic mixture (Fig. 11b) of aluminum and T phase. Point analysis (Table 2) of this T phase showed corrected values of 42.0 wt% zinc, 23.0 wt% magnesium and 35.0 wt% aluminum associating the T phase to $(Al,Zn)_{49Mg32}$. In this case the corrected matrix analysis shows 7.5 wt% zinc and 1.9 wt% magnesium. The composition of the T phase was therefore different in the two alloys, confirming that this phase has a wide range of composition.[14] With the alloy composition and casting conditions used, no formation of a magnesium-zinc intermetallic compound (such as $MgZn_2$) was observed.
The T phase in both alloys was found to oxidize at a slightly faster rate than the matrix and the oxidation product was rapidly dissolved in the electrolyte during the anodizing process (Fig. 11) leaving voids in the anodic films. The small white particles entrapped in the anodic film (Fig. 11b) were unoxidized or only partly oxidized aluminum from the aluminum T phase eutectic regions from which the T phase was oxidized and dissolved resulting in electrical cut-off of the aluminum eutectic component.

Clearer evidence of the rapid dissolution of the oxidized T phase is shown in the series of optical-electron x-ray scanning images (Fig. 12) of an intermetallic particle in the Al-9Mg-3Zn alloy. The slightly faster anodizing rate, of the T phase particles in regards to the matrix, is shown in the electron scanning image (Fig. 12b). The complete dissolution in the electrolyte of the particle in the anodic film is well shown in Figs. 12c and 12d. Figure 12d shows an apparent enrichment of magnesium at the outer edges of the anodic film. This was due to contamination with magnesia, which had to be used in the final stage of preparation in order to show up the particles without actually etching the specimen.

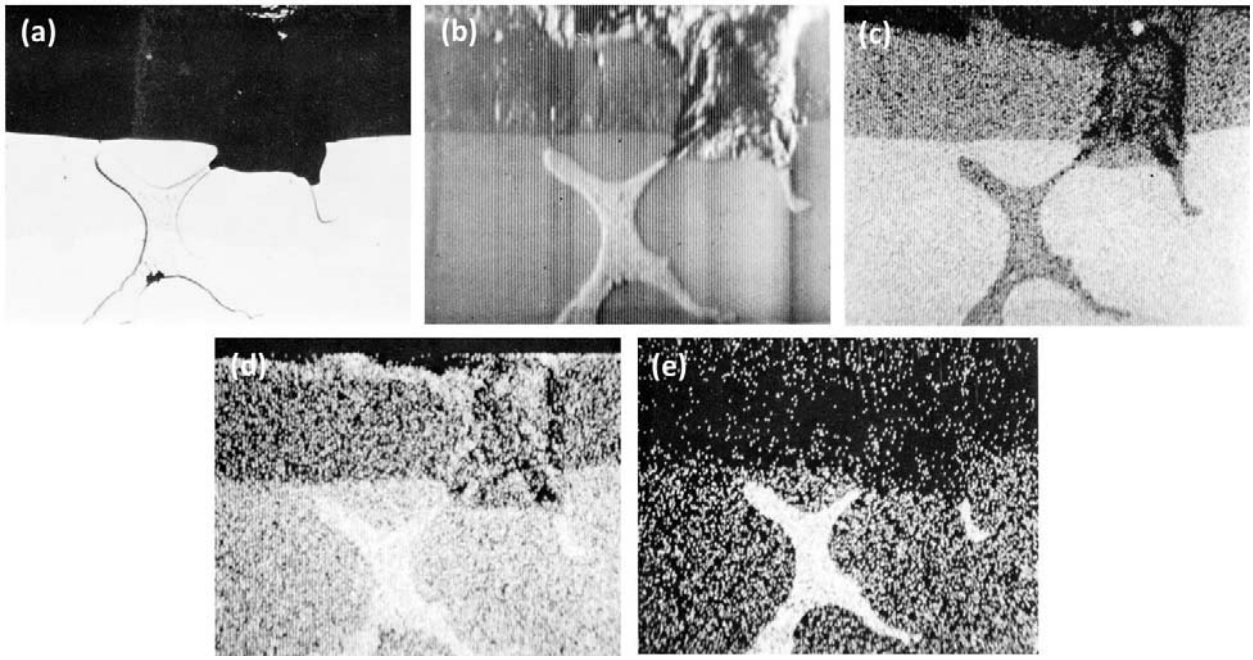

Figure 12 - Cross-section of anodized Al-9Mg-3Zn alloy illustrating the behavior of T (AlZnMg) phase (Original; magnification 300×): (a) optical micrograph, (b) electron scanning image, (c) Al Kα radiation x-ray scanning image, (d) Mg Kα radiation x-ray scanning image and (e) Zn Kα radiation x-ray scanning image.

B. Retention of solute elements in anodic films

By using slowly solidified material, regions free of intermetallic compounds could be selected where the distribution of the alloying elements, in solid solution, through the matrix and the anodic film was determined without possible interference from the intermetallic particles.

The observed static probe analysis data for the elements in the matrix and in the anodic films, for the various alloys, are listed in Table 2 along with the corrected values for the elements in the matrix. In order to obtain some indication of the concentration profile of elements in the anodic films, analysis by the ultra-slow scanning facilities of the instrument was made but only of the single element alloy addition, such as the Al-10Cu, Al-10Mg and Al-13Si alloys.†† As revealed by the concentration profile distribution curves, described below, the concentration of alloying element across anodic films varied somewhat, *i.e.*, decreasing from the oxide/metal through the oxide/electrolyte interfaces. Therefore, the static measurements of the observed concentrations in Table 2 are not truly average concentrations. They represent values rather nearer the oxide/electrolyte interface, where more porous film existed than the oxide/metal interface.

No attempt was made to apply absorption corrections for the anodic film composition, as this would have required, in addition to the aluminum and alloying element concentrations, determination of the amounts of sulfur, oxygen and water or hydrated products present in the film.[8] Even if the amount of oxygen could be measured accurately, it would still be difficult, unless other techniques were used, to tell whether or not the alloying elements are in an oxidized state in the anodic film.

In our work, the observed aluminum content in the anodic film varied between 27 wt% with the Al-10Mg alloy to 31 wt% with the Al-13Si and Al-4Fe-8Si alloys. Wood and Brock[8] reported corrected values of 48 to 52 wt% aluminum, near the oxide/metal interface, where more dilute alloy composition was used than in our investigation. It is interesting to note that the stoichiometric value for aluminum in Al_2O_3 is 53 wt%.

Using the observed electron probe microanalysis values, the aluminum oxide/metal composition ratio for the various alloys was about 0.3. This ratio was used as a criterion for the oxide/metal ratio of the alloying elements and to determine whether the elements were insoluble (ratio equal or higher than 0.3) or soluble (ratio lower than 0.3)[1] as listed in Table 3. Also included in Table 3 is the "solubility" of alloying elements as determined by Spooner[9] and Ramous and Sticchi[10] from x-ray emission spectroscopy of commercial alloys.

Table 3 - "Solubility" of solute elements during sulfuric acid anodizing of aluminum alloys.

			"Solubility" During Anodic Oxidation in H_2SO_4		
Alloy	**Element**	**Oxide/Metal Ratio**	**Present Work**	**Spooner Work[9]***	**Ramous and Sticchi Work[10]****
Al-10Cu	Cu	0.2/3.0 = 0.07	Soluble	Insoluble to Soluble	—
Al-10Mg	Mg	0.5/7.5 = 0.07	Soluble	Partly Soluble	Soluble
Al-13Si	Si	0.6/0.6 = 1.0	Insoluble	Insoluble	Partly Soluble
Al-4Fe-8Si	Fe	trace/0.1 = 0	Soluble	Soluble	Partly Soluble
	Si	0.5/0.5 = 1	Insoluble	Insoluble	Partly Soluble
Al-9Mg-3Zn	Mg	0.6/6.3 = 0.10	Soluble	Partly Soluble	Soluble
	Zn	0.5/2.1 = 0.24	Partly Soluble	Insoluble to Soluble	—
Al-9Zn-3Mg	Mg	trace/1.3 = 0	Soluble	Partly Soluble	Soluble
	Zn	1.1/7.5 = 0.15	Partly Soluble	Insoluble to Soluble	—

*Anodizing done in 15 wt per cent H_2SO_4, 1.6 A/dm² (15 A/ft²).
**Anodizing done in 10 wt per cent H_2SO_4, 1 to 5 A/dm² (9.4 to 42 A/ft²).
NOTE: Spooner and Ramous and Sticchi used commercial alloys.

The concentration profile by simultaneous slow-scan of the aluminum-copper, aluminum-magnesium and aluminum-silicon elements of the Al-10Cu, Al-10Mg and Al-13Si alloys respectively are illustrated in Figs. 13a to 13c. In each case, the concentration values near the interfaces showed a rapid change. This was mainly due to overlapping of the x-ray source with

††No attempt was made to determine the concentration profiles of the Al-Ti and the Al-Fe-Si alloys because in the former alloy no titanium was detected in the anodic film and similarly for iron in the AlFeSi alloy. Silicon in this latter alloy was assumed to have similar behavior to that of silicon in the Al-13 Si alloy. Similarly, no concentration profile was established with the AlZnMg alloys because the interaction of zinc and magnesium on each other during analysis was uncertain and because it has been reported[8] that zinc distribution in anodic film on single alloy addition parallels the behavior of magnesium.

the matrix or the mounting compound, which covered a region of few microns in diameter. It should also be realized that all results are averages over discrete areas.

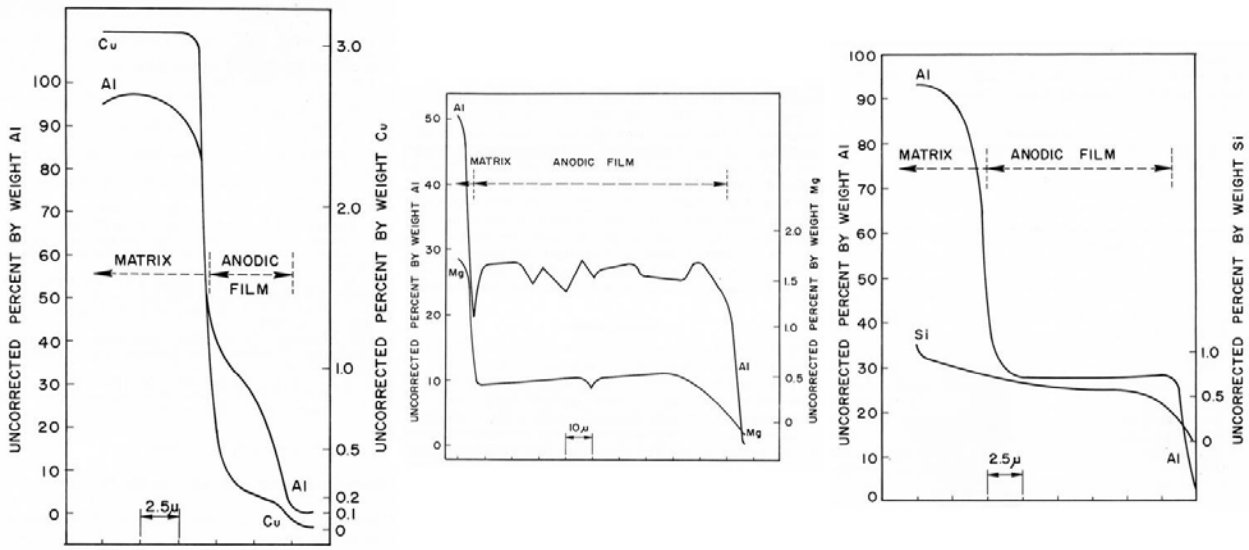

Figure 13 - Concentration profiles through sulfuric acid anodic films of aluminum and alloying elements on (a) Al-10Cu alloy, (b) Al-10Mg alloy and (c) Al-13Si alloy.

With the Al-10Cu alloy (Fig. 13a), although a rather thin anodic film of 6-7 microns was formed, it can be noted that the concentrations of both aluminum and copper more or less rapidly decreased across the anodic film; this was also found by Wood and Brock.[8] The copper and aluminum concentration from the matrix to the anodic film fell rapidly within a very narrow region presumably throughout the barrier layer or in a region adjacent to it. At some distance away, the observed aluminum concentration dropped from about 35 wt% near the metal/oxide interface to about 5 wt% near the oxide/electrolyte interface. The copper concentration, over the same distance, dropped from about 0.3 to 0.1 wt%. The copper/aluminum concentration ratio varied from 0.03 in the metal to 0.01 both near the metal/oxide and oxide/electrolyte interfaces and this also suggests dissolution of copper in the anodic film. Spooner[9] found that copper was insoluble to soluble in the electrolyte depending on the alloy and temper used. The decrease in both aluminum and copper concentrations throughout the anodic film suggests a gradual increase in oxide porosity from barrier layer to the oxide/electrolyte interface.

The slow-scan traces of the aluminum and magnesium through the Al-10Mg alloy anodic film (Fig. 13b) showed both to be fairly constant except, as expected, for a gradual decrease near the oxide/electrolyte interface. The results agreed very well with those of Wood and Brock[8] although they used corrected values. The oxide/metal ratio for the magnesium was 0.07 (Table 3) suggesting leaching out of the magnesium. Also, comparison of the aluminum-magnesium ratio in the metal (7.5/92.5 = 0.08) with that of the anodic film (0.5/27 = 0.02) indicated that magnesium was dissolved in the electrolyte. Spooner and Ramous and Sticchi reported the magnesium to be partly soluble to soluble respectively (Table 3).

The concentration profile of the Al-13Si alloy (Fig. 13c) showed a fairly uniform aluminum concentration while the silicon concentration decreased only very slightly from matrix to anodic film and was also fairly uniform through the anodic film. Based on the observed values, the silicon-aluminum ratio in both the matrix and anodic film and the oxide/metal silicon ratio indicated that silicon was retained in the anodic film. Spooner agreed with our findings while Ramous and Sticchi reported silicon to be partially soluble.

The oxide/metal ratio for the rest of the elements (Table 3) indicated that iron was apparently soluble while silicon was retained in the anodic film in the Al-4Fe-8Si alloy, and both magnesium and zinc were soluble in the electrolyte in the Al-9Mg-3Zn and Al-9Zn-3Mg alloys (Table 3). Spooner and Ramous and Sticchi more or less agreed with our findings, as indicated in Table 3. Only

a trace of titanium was detected in the matrix of the Al-1 Ti alloy so it was impossible to establish whether this element was retained in the anodic film or dissolved in the electrolyte.

Discussion

The sulfuric acid anodic behavior of the coarse inter-metallic compounds investigated revealed that Si, $TiAl_3$ and beta AlFeSi were inert, beta AlMg was oxidized at a slightly faster rate than the matrix and dissolved, while the $CuAl_2$ and the T phase were oxidized and readily dissolved in the electrolyte. The behavior of $CuAl_2$, beta AlMg and Si agrees with the findings of various workers in this field. To our knowledge, it is the first time that the sulfuric acid anodic behavior of $TiAl_3$ and T phase has been reported, although Guminski, *et al*.[5] reported the oxalic acid anodic behavior of $TiAl_3$, which was also inert. Fisher, *et al*.[4] reported that $Al_2Mg_3Zn_3$ (which could be associated with the T phase) was readily dissolved. Keller and his colleagues[3] reported that beta AlFeSi oxidized as rapidly as the aluminum matrix, while we found that these intermetallic compounds were entirely inert. The differences in anodizing conditions between our work and that of Keller, *et al*. were not sufficient to explain the dissimilar behavior unless, in using constant current density, as Keller and his co-workers did, higher voltage is required resulting in some overheating effect and consequently oxidation of the intermetallic compound.

The inert constituents (Si, $TiAl_3$, and beta AlFeSi) became trapped in the anodic films and fractured as a result of the stresses developed by anodic film growth. Pronounced scalloping of the anodic film occurred around these inert particles producing a non-uniform metal/oxide and oxide/ electrolyte interface. The formation of the scalloped interfaces depended on the particle orientation and was probably due to current shielding by these particles rather than to current thieving as suggested by Cooke.[15] In commercial applications, the presence of abundant and uniformly-distributed small particles of these intermetallic compounds can be expected to result in the formation of integrally-colored anodic films. This also applies to the intermetallic compound $MnAl_6$, reported previously.[1] In fact, integrally-colored films are obtained with aluminum-high silicon alloys (AA-4043) and aluminum-manganese alloys (AA-3003) by anodizing in sulfuric acid as well as other types of electrolytes.

For those intermetallic compounds that were attacked, there was some evidence from the x-ray scanning images that the actual dissolution in the electrolyte was preceded by oxidation. This can be seen in the $CuAl_2$ scanning images (Fig. 2). Those intermetallic compounds that were oxidized and dissolved more rapidly than the matrix ($CuAl_2$, beta AlMg and T phase) showed only small scalloping effect of the anodic film around the particles. It appeared that, in these cases, current thieving[15] by the intermetallic compounds was responsible for the scalloping effect.

Of the intermetallic compounds studied so far, those formed with manganese,[1] silicon, titanium, and iron-silicon (beta AlFeSi) were inert; those formed with iron[1] were oxidized, while those formed with chromium,[1] copper, magnesium, magnesium-silicon,[1] and zinc-magnesium were oxidized and dissolved. The exact relationship or relationships which determine the inertness or reactivity of individual intermetallic compound, for a given set of anodizing conditions, is not too clear. The crystallographic structure of the intermetallic compounds, their atomic bonding strength, atomic radius, electrode potentials, the degree of ionization under an electrical field, the solubility in the electrolyte of their reaction products, must be interrelated to some extent, determining whether an intermetallic compound is inert, oxidized, oxidized and dissolved, or possibly just dissolved in the electrolyte. Attempts to find correlation between normal electrode potential,[8] crystallographic structure or atomic radius did not show a definite pattern to explain fully which intermetallic compounds should be inert or oxidized.

The use of observed chemical composition, from the ultra-slow scan of the electron probe microanalyzer, to establish the concentration profile and thereafter determine whether the solute elements were retained or dissolved in the anodic film is to some extent open to question. However, even if correction for absorption was made, this will not appreciably affect the general findings. Indeed, Wood and Brock[8] reported a corrected aluminum content in the anodic film of about 50 wt% which would be about the same for the alloys used in our investigation. Therefore the criterion for retention or dissolution based on the corrected aluminum oxide/metal ratio[1] would be approximately 0.5. Even if correction had been made for the alloying elements in the anodic film, their oxide/metal ratios would not have been greatly different from those based on the observed composition values and consequently the classification of the elements according to whether they are retained or dissolved would be about the same.

As is the case for intermetallic compounds, it is of interest to consider why solute elements are either retained or dissolved during the anodic process and what mechanisms are responsible. In either case, how are the structure and properties of the anodic film affected? Wood and Brock[8] suggested that the incorporation of elements in the anodic film may possibly promote hydration of the anodic film or different crystallographic oxide forms resulting in an anodic film that could be more or less soluble. In cases where dissolution occurs, more porous films might be produced and the properties of the resulting anodic film could be affected. As yet, little is known about such changes, but there may be circumstances when such changes could be significant and this is an area where some further work could be beneficial.

Conclusion

By the use of electron probe microanalysis, it was found or confirmed that, during sulfuric acid anodizing, particles of Si, $TiAl_3$, and beta AlFeSi are inert, while particles of $CuAl_2$, beta AlMg and the T phase anodize faster than the aluminum matrix and are dissolved readily in the electrolyte. However, the anodizing behavior of large intermetallic compounds studied in this work, using high purity base aluminum alloys, may not be identical to that of similar constituents occurring in commercial alloys because such alloys are usually of lower purity. The elements in solid solution also respond differently during anodizing. Silicon is retained in the anodic film, zinc is partly dissolved, while copper, iron and magnesium are largely dissolved in the electrolyte.

References

1. J. Cote, E.E. Howlett, M.J. Wheeler and H.J. Lamb, *Plating*, 56, 386 (1969).
2. F. Keller and G. W. Wilcox, *Metals and Alloys*, 10 (6), 187 (1939).
3. F. Keller and G.W. Wilcox, M. Tosterud and C.D. Slunder, *ibid*., 10 (7), 219 (1939).
4. M. Fisher, M. Budiloff and L. Kock, *Korrosion u. Metallschutz*, 16 (718), 236 (1940).
5. R.D. Guminski, P.G. Sheasby and H.J. Lamb, *Trans. Inst. Metal Finishing*, 46, 44 (1968).
6. J. Herenguel and P. LeLong, *Metal Finishing J. (London)*, 4 (1), 20 (1958).
7. P. Lacombe and L. Beaujard, *Metal Treat.*, 12 (44), 223 (1945).
8. G.C. Wood and A.J. Brock, *Trans. Inst. Metal Finishing*, 44, 189 (1966).
9. R.C. Spooner, *Plating*, 53, 451 (1966).
10. E. Ramous and P. Sticchi, *Alluminio*, 36 (5), 247 (1967).
11. S. Wernick and R. Pinner, *The Surface Treatment and Finishing of Aluminium and its Alloys*, Robert Draper Ltd., Teddington, U.K.. 1964; Chapter 7.
12. G.H. Kissin, *Finishing of Aluminum*, Reinhold Publishing Corp., New York, NY, 1963; Chapter 2.
13. G.C. Wood, V.J.J. Marron and B.W. Lambert, *Nature*, 199 (7), 239 (1963).
14. The Aluminum Development Association, *Equilibrium Diagrams of Aluminum Alloy Systems*, *Information Bulletin*, 25, 24 (1961).
15. W.E. Cooke, *Plating*, 49, 1157 (1962).
16. L.S. Birks, *Electron Probe Microanalysis*, Interscience Publishers, New York, NY, 1963.

About the authors

J. Cote is a research metallurgist with Alcan Research and Development Limited, Kingston, Ontario, Canada, engaged in the finishing field of aluminum. He obtained an honours BSc in metallurgical engineer¬ing from Ecole Polytechnique - University of Montréal. In 1961 he joined the Aluminum Company of Canada at Shawinigan, Québec, but in 1933 transferred to Aluminum Laboratories (now Alcan Research and Development Limited). He has had experience in various aspects of finishing with special interest in alkaline etching and the mechanism of formation and ageing of anodic films.

E.E. Howlett is a research metallurgist engaged in research and development at Alcan Research and Development Limited, Kingston, Ontario, Canada. He joined Alcan in 1953 and obtained his degree in metallurgical engineering at Queen's University, Kingston, in 1960. For the past eight years he has specialized in studying surface finishing of aluminum alloys particularly anodizing and porcelain enameling finishes.

H.J. Lamb joined Northern Aluminium Company Limited (now Alcan Industries Limited) at Banbury, England, U.K., in 1948. He transferred to Aluminium Laboratories Limited (now Alcan Research and Development Limited) in 1953 where he is now employed on the electron probe microanalyzer. Previously he was concerned in developing techniques for growing single crystals in aluminum and aluminum alloys and in zone refining aluminum.